Am J Cancer Res 2021;11(6):2893-2910
www.ajcr.us /ISSN:2156-6976/ajcr0125036

Original Article

Integrative multiplatform-based molecular profiling of human colorectal cancer reveals proteogenomic alterations underlying mitochondrial inactivation

Wei Zhang[1,2], Donge Tang[1], Liewen Lin[1], Tingting Fan[6], Ligang Xia[1], Wanxia Cai[1], Weier Dai[3], Chang Zou[1], Lianghong Yin[4], Yong Xu[5], Yong Dai[1]

[1]Department of Clinical Medical Research Center, The Second Clinical Medical College, Jinan University (Shenzhen People's Hospital), Shenzhen 518020, China; [2]The First Affiliated Hospital, Jinan University, Guangzhou, China; [3]College of Natural Science, University of Texas at Austin, Austin 78721, United States of America; [4]Department of Nephrology, Institute of Nephrology and Blood Purification, The First Affiliated Hospital of Jinan University, Jinan University, Guangzhou 510632, China; [5]The First Affiliated Hospital of Shenzhen University, Shenzhen Second People's Hospital, Shenzhen 518028, China; [6]State Key Laboratory of Chemical Oncogenomics, Key Laboratory of Chemical Biology, Tsinghua Shenzhen International Graduate School, Tsinghua University, Shenzhen 518055, China

Received October 27, 2020; Accepted April 14, 2021; Epub June 15, 2021; Published June 30, 2021

Abstract: Mitochondria play leading roles in initiation and progression of colorectal cancer (CRC). Proteogenomic analyses of mitochondria of CRC tumor cells would likely enhance our understanding of CRC pathogenesis and reveal new independent prognostic factors and treatment targets. However, comprehensive investigations focused on mitochondria of CRC patients are lacking. Here, we investigated global profiles of structural variants, DNA methylation, chromatin accessibility, transcriptome, proteome, and phosphoproteome on human CRC. Proteomic investigations uncovered greatly diminished mitochondrial proteome size in CRC relative to that found in adjacent healthy tissues. Integrated with analysis of RNA-Seq datasets obtained from the public database containing mRNA data of 538 CRC patients, the proteomic analysis indicated that proteins encoded by 45.5% of identified prognostic CRC genes were located within mitochondria, highlighting the association between altered mitochondrial function and CRC. Subsequently, we compared structural variants, DNA methylation, and chromatin accessibility of differentially expressed genes and found that chromatin accessibility was an important factor underlying mitochondrial gene expression. Furthermore, phosphoproteomic profiling demonstrated decreased phosphorylation of most mitochondria-related kinases within CRC versus adjacent healthy tissues, while also highlighting MKK3/p38 as an essential mitochondrial regulatory pathway. Meanwhile, systems-based analyses revealed identities of key kinases, transcriptional factors, and their interconnections. This research uncovered a close relationship between mitochondrial dysfunction and poor CRC prognosis, improve our understanding of molecular mechanism underlying mitochondrial linked to human CRC, and facilitate identifies of clinically relevant CRC prognostic factors and drug targets.

Keywords: Mitochondria, multi-omics, colorectal cancer, prognosis, drug targets

Introduction

Colorectal cancer (CRC) is the fourth deadliest type of cancer worldwide. It kills nearly 900,000 people each year and accounts for 10% of all cancer deaths [1]. Although new promising treatments, such as targeted and immune therapies, have become available in recent years [2, 3], the CRC mortality rate still exceeds 40% per year [4], with approximately 50% of patients experiencing recurrence and distant metastasis during disease progression [5]. Thus, a better understanding of the molecular basis of CRC is needed for promoting practical therapeutics and diagnosis.

As vital eukaryotic organelles, mitochondria play critical roles in CRC initiation and development [6-8]. In early-stage CRC, metabolic changes resulting from mitochondrial depletion are at the foundation of cellular transformation [6, 9]. Simultaneously, tumor develop-

ment requires reactivation of mitochondrial functions to support cell proliferation and metastasis [6]. At present, mitochondria have attracted attention as potential drug targets due to their indispensable roles in energy generation, apoptosis, and metabolism [8]. Notably, proteogenomic profiling of mitochondria would provide valuable information to facilitate discovering new cancer treatment targets and understanding molecular mechanisms underlying the occurrence and progression of CRC [10-12]. However, such comprehensive investigations in human are lacking.

In this study, we conducted a multiplatform omics-based analysis of mitochondria in cells of cancerous and adjacent non-cancerous tissues of CRC patients (n = 6-8) to obtain original data to reveal CRC-based differences with respect to structural variants, DNA methylation, chromatin accessibility, as well as proteomic and phosphoproteomic profiles. Using our original data combined with RNA-Seq datasets of CRC patients (n = 538) obtained from The Cancer Genome Atlas (TCGA), relationships were uncovered between mitochondrial characteristics and CRC patient outcomes. Furthermore, we identified key transcriptional factors and kinases, as well as their functional interconnectivity with possible relevance to the regulation of mitochondrial activities.

Materials and methods

Patients

Patients with primary CRC admitted to Shenzhen People's Hospital who had undergone surgical resection without prior radiotherapy or chemotherapy were eligible for inclusion in this study. Patients with hereditary CRC were excluded. Gastroenterologists graded each case based on pathologic analysis. Clinical information, pathological features, and treatment information were obtained from patients' electronic medical records. All study participants were informed and signed informed consent forms after they were told that their participation was voluntary. This project was approved by the ethical committee of Shenzhen People's Hospital (LL-KY-2019213).

Protein extraction and digestion

Tissues of CRC patients were collected using a previously reported method [13]. In short, tumor tissues removed from CRC patients were collected within 1 hour after surgery. Both tumor and normal adjacent tissues were obtained from the colon segment, with normal adjacent colorectal mucosa harvested at a distance of 5 cm from the tumor. Samples were placed in liquid nitrogen for at least 3 hours then were stored at -80°C. Tissue samples frozen in liquid nitrogen were ground into powder then were mixed with four volumes of lysis buffer containing 8 M urea and 1% protease inhibitor cocktail (Merck Millipore, 156535140). The resulting mixture was sonicated three times on ice using a high-intensity ultrasonic processor (Scientz, China) then the debris was removed via centrifugation at 12,000 × g at 4°C for 10 min. Finally, the supernatant was collected and the protein concentration was determined using a BCA kit (P0011-1, Beyotime, China) according to the manufacturer's instructions. The protein-containing sample was then incubated with 5 mM dithiothreitol at 56°C for 30 min then was mixed with 11 mM iodoacetamide and incubated at room temperature in darkness for another 15 min. Next, 100 mM TEAB was added to reduce the urea concentration to less than 2 M. Then, the mixture was incubated with trypsin at a 1:50 ratio for 12 h for the first-round digestion, followed by incubation with a 1:100 ratio of trypsin for 4 h for the second-round digestion.

LC-MS/MS analyses

LC-MS/MS analyses were conducted using a standard protocol [14]. The timsTOF Pro, a quadrupole time-of-flight mass spectrometer with a modified nano-electrospray ion source (Bruker Daltonics, MA, USA), was used for all experiments and was run using a parallel accumulation-serial fragmentation (PASEF) mode. Tryptic peptides were dissolved in 0.1% formic acid (solvent A), directly loaded onto a homemade reversed-phase analytical column (15-cm length, 75-μm i.d. for proteomic analyses and 25-cm length, 100-μm i.d. for phosphoproteomic analyses). Proteomic analysis was conducted as follows: for the first 70 min, the solvent gradient was increased from 6% to 24% by addition of solvent B (98% acetonitrile with 0.1% formic acid) then increased again from 24% to 35% over 14 min, further increased to 80% over 3 min, then maintained at 80% for an additional 3 min. For phosphoproteomic analysis, the gradient was increased gradually over

50 min from 2% to 22% by addition of solvent B (acetonitrile with 0.1% formic acid) then was increased again from 22% to 35% over 2 min, then increased to 90% over 3 min, then was maintained at 90% for 5 min. All steps were implemented using a constant flow rate of 450 nL/min using a nanoElute UPLC system (Bruker Daltonics). Next, peptides were transferred to a glass capillary tube and processed using timsTOF Pro mass spectrometry using an applied electrospray voltage of 1.6 kV. Precursors and fragments were measured and analyzed using the TOF detector, with MS/MS scanning conducted across the range of 100 to 1700 m/z. Precursors with charge states from 0 to 5 were selected for fragmentation, 10 PASEF-MS/MS scans were acquired per cycle, and dynamic exclusion was set to 30 s.

MS/MS data were analyzed using the Maxquant software package (v1.6.6.0). The reference database Homo_sapiens_9606_SP_201911-15 (20380 sequences) was used, and a reverse library was added to calculate the false positive rate caused by random matching. In addition, common contamination libraries were added to the database to eliminate the influence of contaminating proteins from the results. The method of enzyme digestion was set to Trypsin/P, and the number of missed sites was set to 2. The minimum peptide length was set to 7 amino acid residues, and the maximum modification number of peptides was set to 5. Mass tolerances for precursor ions in the first search and main search were each set to 20 PPM, and for fragment ions was set to 0.02 Da. The alkylation of cysteine was set as a fixed modification, and the variable modification was set to methionine oxidation (for phosphoproteomic analysis, carbamidomethyl on Cys was selected as the fixed modification, while oxidation of Met, acetylation of N-termini of proteins, and phosphorylation of Ser, Thr, Tyr residues were regarded as variable modifications). Finally, the false discovery rate (FDR) and peptide-spectrum match (PSM) were set to 1%.

Protein annotation and functional enrichment

The UniProt-GOA database was used for Gene Ontology (GO) annotation with InterProScan (an algorithm based on protein sequences). For Kyoto Encyclopedia of Genes and Genomes (KEGG) pathway annotation, identified proteins were primarily annotated using KAAS v.2.0 (KEGG online tool), then KEGG mapper V2.5 was used to assign proteins to KEGG pathways. Finally, subcellular enrichment was performed using WoLFPSOR v.0.2 software.

TCGA data

Level 3 RNA-Seq datasets of 51 healthy people and 647 CRC patients were downloaded from the TCGA database, followed by the removal of data from subjects with unknown survival times. Ultimately, a total of 538 sample data files were included in the study by initially merging single files into a matrix file. Next, gene names were converted from Ensembl IDs to gene symbols based on Ensembl database documentation then datasets of healthy subjects and CRC patients were extracted from the symbol matrix. The R package module "survival" v.2.4.2 was used for both survival analyses and progression-free survival analyses (PFS) using a log-rank method. Independent prognostic factor (IPF) genes were screened using Cox regression analysis.

Assay to detect transposase-accessible chromatin based on high throughput sequencing (ATAC-Seq)

The ATAC-Seq procedure was performed following a standard reported approach [15]. In short, tissues were digested to yield single cells, and 50,000 cells were collected for the next step. After cells were broken open by the addition of lysis buffer (0.1% IGEPAL CA-630, 3 mM $MgCl_2$, 10 mM NaCl, 10 mM Tris-HCl, pH 7.5), samples were centrifuged at 500 g at 4°C for 10 min then supernatants were removed, and remaining debris was suspended in reaction buffer (2.5 μl of Tn5 transposase and 1 × TD buffer in 50 μl total) followed by incubation at 37°C for 30 min. Next, DNA was purified using a MinElute Reaction Cleanup Kit (QIAGEN, 51306). DNA libraries were generated using the TruePrep™DNA Library Prep Kit V2 for Illumina (Vazyme Biotech, TD501/TD502/TD503), and library quality was verified via real-time PCR tests using the StepOnePlus™ Real-Time PCR System. Lengths of inserted fragments were measured using the HS 2100 Bioanalyzer (Agilent). The resulting high-quality library was sequenced using the HiSeq X Ten sequencing platform (Illumina) based on 150-bp paired-end reads. Raw results were stored in FASTQ format, including base sequences and

corresponding quality control information. Clean data obtained by removing low-quality and adaptor-contaminated reads, then reads were mapped to the corresponding reference genome using Bowtie2. The results were visualized using Integrative Genomics Viewer (IGV), and peaks within open regions of the genome were called using MACS2.

Whole genome bisulfite sequencing (WGBS)

High-quality DNA was prepared using a SMRTbell Express Template Prep Kit 2.0 (Pacific Bioscience, 100-938-900); 1 μg of DNA was used for library construction. C-T conversion was achieved using the EZ DNA Methylation-Gold™ Kit (ZYMO research, D5005). After library construction was complete, a Qubit 2.0 fluorometer (Qubit) was employed for preliminary DNA quantification then the library insert size range was determined using a 2100 Bioanalyzer (Agilent). Subsequently, real-time PCR assays conducted with the StepOnePlus™ Real-Time PCR System were performed to measure the effective concentration of the library (> 10 nM). Finally, the validated library was sequenced using the HiSeq X10 sequencing platform (Illumina), which generated paired-end 150-bp reads.

Long-read whole genome sequencing

High-quality DNA was obtained as described above. A g-TUBETM (Covaris, 520079) was used to break the DNA into fragments of lengths ~20 kb that were then enriched using magnetic beads (Pacific Bioscience, 100-317-100). After adding stem-loop joints to DNA fragments, the new-created fragments went through a second round of screening. Subsequently, the resulting DNA was annealed to primer then sequences were synthesized using DNA polymerase (Pacific Bioscience, 101-731-100). DNA quality was evaluated using a 2100 Bioanalyzer (Agilent) then the validated library was sequenced to generate paired-end 150-bp reads using the Hiseq X10 sequencing platform (Illumina).

Statistical analyses

T tests were used to determine the significance of differential mRNA, protein, and phosphorylation analyses. Fisher's exact tests were used to evaluate the significance of enrichment results. Cox regression analyses were performed on expression datasets to obtain *p* values of risk scores for the IPFs. *P* values < 0.05 were considered significant.

Availability of data and materials

Mass spectrometry proteomics and phosphoproteomics data have been unloaded and deposited into the ProteomeXchange Consortium through the PRIDE partner repository as entries designated PXD021314 and PXD021318. Data of ATAC-Seq, WGBS, and long-read whole-genome sequencing results obtained in this study have been unloaded and deposited into the Sequence Read Archive (SRA) with accession to PRJNA693028. All script codes have been uploaded as Supplementary Materials.

Results

Proteome-transcriptome analyses revealed mitochondrial inactivation in human CRC that was strongly associated with patient prognosis

To understand the association between mitochondrial proteogenomic alterations in CRC patients, intestinal epithelial tissues of CRC patients were collected then were subjected to multiplatform analysis that included assessments of structural variants, DNA methylation, chromatin accessibility, and determinations of proteomic and phosphoproteomic profiles (**Figure 1A**). Samples of CRC tumor tissues and adjacent normal tissues were surgically obtained from colonic adenocarcinoma patients (n = 8), including four patients with early-stage (I-II) CRC and four patients with late-stage (III-IV) CRC (**Table 1**). Samples from two patients of each disease stage were pooled then tested.

First, to reveal differentially expressed mitochondrial proteins, we conducted label-free proteomic experiments using a high-throughput timsTOF Pro platform. As a result, a total of 1093 differentially expressed genes based on comparisons between CRC tissues and normal adjacent tissues were identified, of which 496 were up-regulated and 597 were down-regulated in CRC tissues (fold change > 1.5, P < 0.05) (Figure S1). Next, we annotated the 1093 genes based on GO, KEGG, and subcellular location

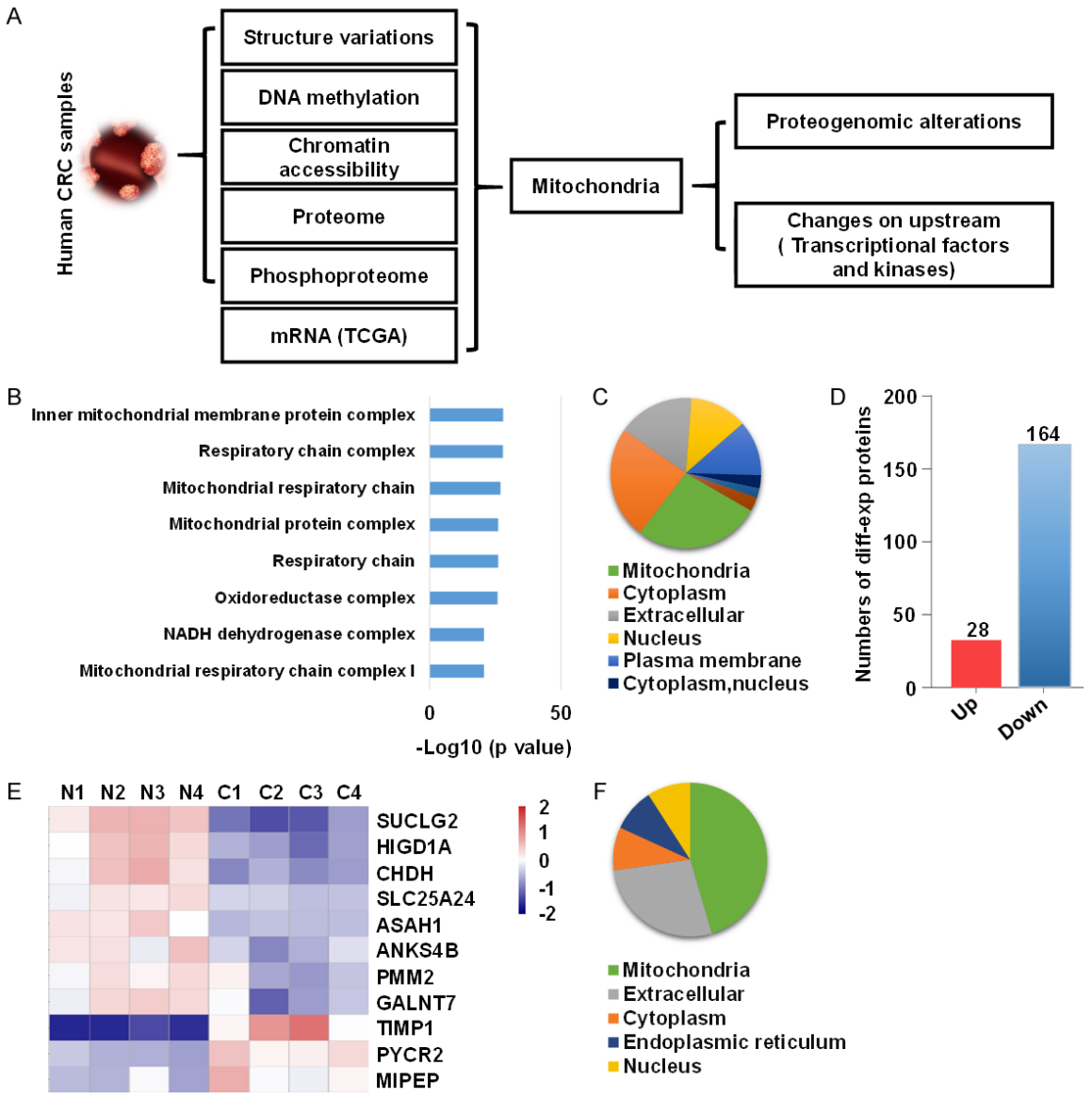

Figure 1. Transcriptome-proteome analyses demonstrated that mitochondrial dysfunctions were highly relevant to CRC patient outcomes. (A) Schematic overview of this study. (B) GO and (C) subcellular enrichment of differentially expressed genes. (D) 164 of 192 differentially expressed mitochondrial proteins were down-regulated in CRC. Genes with fold change > 1.5 were regarded as differentially expressed genes. (E) Heat map showing protein levels of 11 IPFs in normal adjacent tissues and CRC tissues after protein levels were analyzed via proteomic analyses. "N" indicates normal adjacent tissues and "C" indicates cancer tissues. (F) Subcellular enrichment of CRC-associated IPFs revealing that 45.5% of IPFs were mainly localized within mitochondria.

analyses. Surprisingly, the top eight identified cellular components were all associated with mitochondria, including inner mitochondrial membrane protein complex, respiratory chain complex, mitochondrial respiratory chain, mitochondrial protein complex, respiratory chain, oxidoreductase complex, NADH dehydrogenase complex, and mitochondrial respiratory chain complex I (**Figure 1B**). Moreover, the top three pathways that were most altered in CRC tissues relative to adjacent normal tissues were all relevant to mitochondria, including oxidative disease, Parkinson's disease, and Alzheimer's disease (Figure S2) [16]. In addition, subcellular analyses revealed that expression-altered proteins exhibited more mitochondrial proteins than other organelles (27% of all differentially expressed proteins) (**Figure 1C**).

Table 1. The characteristics of eight CRC patients in our study

		I-II	III-IV
Age	≤ 65	0 (0.0%)	1 (12.5%)
	> 65	4 (50.0%)	3 (37.5%)
Type	Adenocarcinoma	4 (50.0%)	4 (50.0%)
Sex	Male	1 (12.5%)	3 (37.5%)
	Female	3 (37.5%)	1 (12.5%)
T-stage	T1	1 (12.5%)	0 (0.0%)
	T2	0 (0.0%)	0 (0.0%)
	T3	2 (25.0%)	1 (12.5%)
	T4	1 (12.5%)	3 (37.5%)
N-stage	N0	4 (50.0%)	0 (0.0%)
	N1	0 (0.0%)	4 (50.0%)
	N2	0 (0.0%)	0 (0.0%)
M-stage	M0	4 (50.0%)	1 (12.5%)
	M1	0 (0.0%)	3 (37.5%)
Location	Ascending colon	2 (25.0%)	1 (12.5%)
	Sigmoid colon	1 (12.5%)	3 (37.5%)
	Appendix colon	1 (12.5%)	0 (0.0%)
Chemotherapy	Yes	0 (0.0%)	0 (0.0%)
	No	4 (50.0%)	4 (50.0%)

Table 2. The characteristics of 538 CRC patients from TCGA

	Type	Patients
Fustat	Alive	431 (80.1%)
	Dead	107 (19.9%)
Age	≤ 65	232 (43.1%)
	> 65	306 (56.9%)
Sex	Male	254 (47.2%)
	Female	284 (52.8%)
Stage	I	95 (17.7%)
	II	208 (38.7%)
	III	149 (27.6%)
	IV	86 (16.0%)
T-stage	T1	17 (3.2%)
	T2	92 (17.1%)
	T3	372 (69.1%)
	T4	57 (10.6%)
M-stage	M0	452 (84.0%)
	M1	86 (16.0%)
N-stage	N0	313 (58.2%)
	N1	128 (23.8%)
	N2	97 (18.0%)

Next, after enumeration of all mitochondrial proteins with altered expression, 164 of 192 proteins were found to be down-regulated in CRC tissues (85.4%) (**Figure 1D**). According to previous reports, the collective reduction of mitochondrial proteins in CRC tissues relative to normal tissues reflected decreased mitochondrial activities [6, 9]. Notably, the large loss of mitochondrial proteins in CRC tissues versus healthy tissues highlights the essential role of mitochondrial dysfunction in CRC.

In order to explore the association between mitochondrial factors and CRC patient outcomes, we searched the public database for IPF genes among differentially expressed mRNAs between CRC patients and healthy subjects. First, transcriptomic datasets and survival data of 538 CRC patients (**Table 2**) and 51 healthy people were downloaded from TCGA, then differentially expressed genes, survival-related genes and the IPFs were analyzed. As a result, 16115 genes were found to be differentially expressed in CRC versus healthy patients, with 537 genes found to be associated with overall survival (OS) rate and 203 of these genes identified as IPFs (Table S1). Next, after identifying IPFs among these 203 IPFs that overlapped with our proteomic results, we ultimately identified 11 CRC-associated IPFs (**Figure 1E**). Subcellular analyses revealed that among the 11 IPFs, mitochondrial proteins were the most common, accounting for 45.5% (**Figure 1F**). These results demonstrate that expression of mitochondrial genes had not only undergone extreme changes in CRC cells versus adjacent healthy cells, but that mitochondrial alterations were closely linked to poor CRC patient prognosis.

Characterization of proteogenomic changes underlying mitochondrial impairments in CRC patients

The abovementioned investigations suggest that mitochondria play important roles in CRC development and subsequently influence CRC patient outcomes. Thus, a proteogenomic picture of mitochondria would facilitate screening efforts for discovery of drug targets, while also enhancing our understanding of CRC pathogenesis. Therefore, we analyzed our original data to characterize global structural variants (n = 6), DNA methylation alterations (n = 6), chroma-

tin accessibility differences (n = 6), and phosphoproteomic alterations (n = 8) of CRC patients relative to controls (Table S1). Subsequently, 67 and two nuclear-coding mitochondrial genes (NCMGs) were shown to have structural variants in non-exonic and exonic regions, respectively (**Figure 2A**); promoters of eight and 18 NCMGs were shown to be hyper- and hypomethylated, respectively (**Figure 2B**); chromatin accessibility levels of 146 and 49 NCMGs were increased and decreased, respectively (**Figure 2C**); mRNAs of 469 and 234 NCMGs were up-regulated and down-regulated, respectively (**Figure 2D**); proteins of 28 and 164 NCMGs were up-regulated and down-regulated, respectively (**Figure 2E**); nine and seven NCMGs were hyper- and hypo-phosphorylated, respectively (**Figure 2F**). As is well known, structural variants, DNA methylation of promoters, and alterations of chromatin accessibility influence mRNA transcription, prompting us to use Venn analyses to discover differentially expressed genes with these types of genomic or epigenetic changes. The results demonstrated that among 66 genes with structural variants, expression levels of 39 genes were altered (59.1%) (**Figure 2G**). Among 24 genes with altered methylation, expression levels of nine genes were altered (37.5%) (**Figure 2H**). For 190 genes with altered chromatin accessibility, expression levels of 127 genes were altered (66.8%) (**Figure 2I**), thus implying that chromatin accessibility was strongly linked to expression of NCMGs. Moreover, we investigated effects of the genomic and epigenetic alterations on OS-evaluated NCMGs. Among 537 survival-relevant genes pinpointed in foregoing studies, 33 genes were NCMGs. As shown in **Figure 2J**, **2K**, no distinct structural variants or DNA methylation modifications were found in 33 OS-related NCMGs, although five genes displayed altered chromatin accessibility, including *TFB1M*, *CHDH*, *MIPEP*, *PYCR2*, and *LARS2* (**Figure 2L**). This result suggests that effects of altered chromatin accessibility of NCMGs in CRC patients were closely tied to patient survival. In addition, phosphorylation of PAICS at Ser27 was found to be up-regulated (**Figure 2M**).

Comprehensive analyses disclosed essential transcriptional factors involved in regulation of mitochondria in CRC

As is well known, transcriptional factors regulate transcription of genes. In the abovementioned results, mRNAs of large numbers of NCMGs were shown to be altered in CRC, prompting us to investigate whether their upstream transcriptional factors were also improperly modified, as detected via proteogenomic- or epigenetic-level analysis. First, we identified all experimentally confirmed transcriptional factors downloaded from the hTFtarget database and discovered a total of 511 transcriptional factors for the 703 differentially expressed NCMGs (Table S1). Because transcriptional factors regulate transcription by binding to DNA sequence motifs, we primarily investigated motifs of the 511 transcriptional factors by searching global chromatin accessibility of the two groups.

As a result, the chromatin accessibility of CRC samples was dramatically decreased, with an average peak number of 361,364 (normal) vs. 43,038 (CRC), ratio = 8.40 (Figure S3). Subsequently, we found that binding motifs of SP1, SP2, KLF5 and GLIS1 were inaccessible in CRC patients, but they regulated 75.6%, 86.8%, 82.9% and 91.9%, respectively, of all the down-regulated NCMGs. Meanwhile, binding sites for JUN were more accessible in the CRC group and potentially regulated 90.0% of 469 up-expressed NCMGs (Table S1; **Figure 3A-D**). Next, we also examined protein levels (**Figure 3E**) and phosphorylation levels (**Figure 3F**) of the 511 transcriptional factors. As a result, SUMO2, NKFB2, FOXK1, PML, STAT1, STAT2, YAP1, CDX2, HSF1, OGT, DDX5, YY1, XRN2 showed increased protein levels (**Figure 3E**); of these, NFKR2, YAP1, and YY1 targeted 88.5%, 59.1%, and 48.4% of up-regulated NCMGs, respectively (**Figure 3G**). Meanwhile, CRBE1, SMARCA4, YAP1, PRKDC, FOXK1, XRN2, MYH11, ARRB1, CBX3, ARID1A, LMNB1, HCFC1, RING1 exhibited changed phosphorylation levels (**Figure 3F**), and CREB1, ARID1A, CDK12, and LMNB1 targeted 96.3%, 72.4%, 69.7%, and 67.7%% of differentially expressed NCMGs (**Figure 3H**). Ultimately, we checked for overlapping transcriptional factors of the above three analyses, and found *YAP1*, *STAT2*, *XRN2*, and F*OXK1* were discovered within two omics-based analyses. The intersection results implied that these transcription factors might have greater relevance to CRC mitochondrial dysregulation than did other transcription factors (**Figure 3I**, **3J**). Taken together, these results highlight key transcriptional factors likely involved in CRC-associated mitochondrial dys-

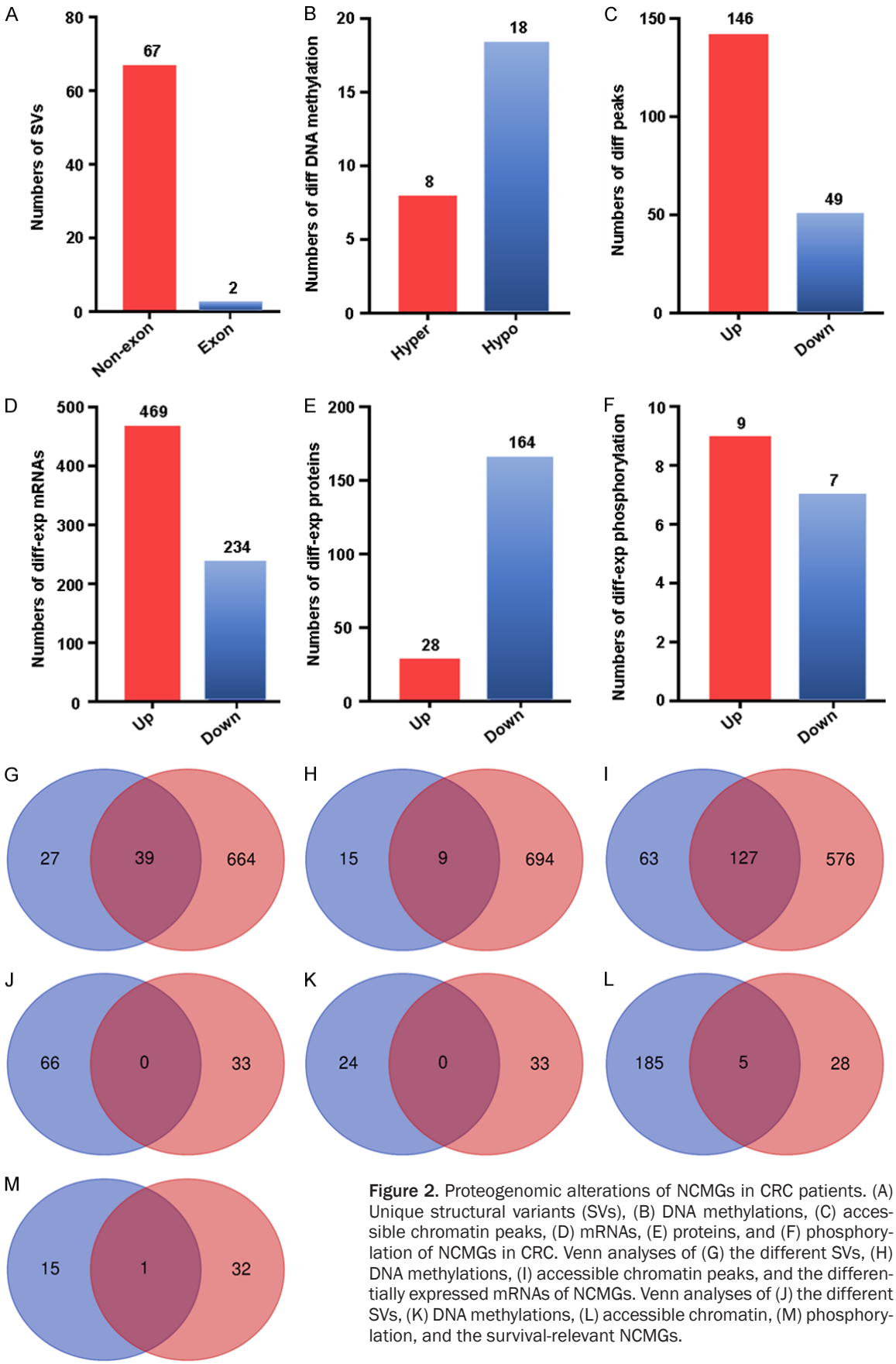

Figure 2. Proteogenomic alterations of NCMGs in CRC patients. (A) Unique structural variants (SVs), (B) DNA methylations, (C) accessible chromatin peaks, (D) mRNAs, (E) proteins, and (F) phosphorylation of NCMGs in CRC. Venn analyses of (G) the different SVs, (H) DNA methylations, (I) accessible chromatin peaks, and the differentially expressed mRNAs of NCMGs. Venn analyses of (J) the different SVs, (K) DNA methylations, (L) accessible chromatin, (M) phosphorylation, and the survival-relevant NCMGs.

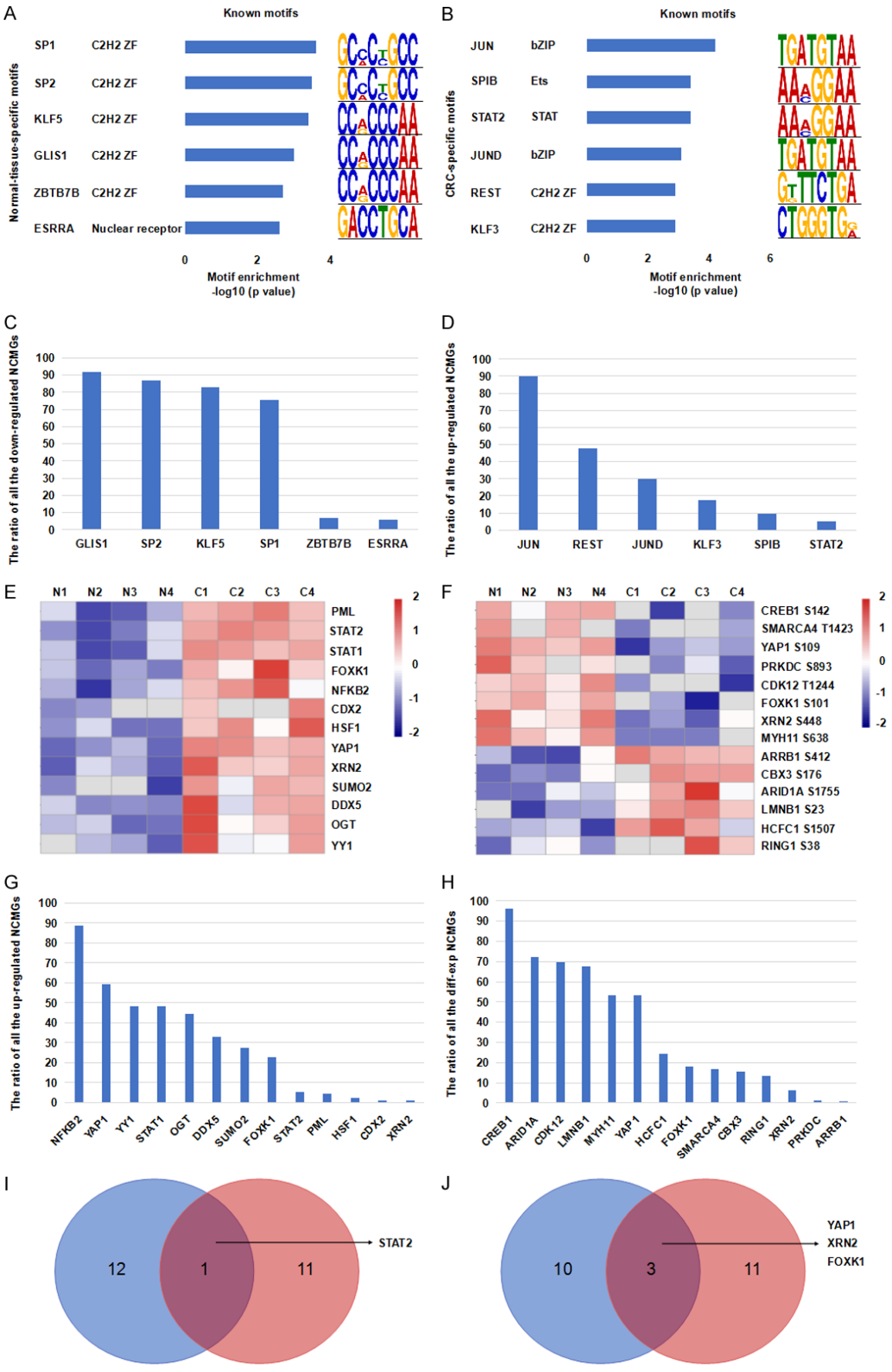
A
Known motifs
Normal-tissue-specific motifs
SP1 C2H2 ZF
SP2 C2H2 ZF
KLF5 C2H2 ZF
GLIS1 C2H2 ZF
ZBTB7B C2H2 ZF
ESRRA Nuclear receptor
0 2 4
Motif enrichment -log10 (p value)
B
Known motifs
CRC-specific motifs
JUN bZIP
SPIB Ets
STAT2 STAT
JUND bZIP
REST C2H2 ZF
KLF3 C2H2 ZF
0 2 4 6
Motif enrichment -log10 (p value)
C
The ratio of all the down-regulated NCMGs
GLIS1 SP2 KLF5 SP1 ZBTB7B ESRRA
D
The ratio of all the up-regulated NCMGs
JUN REST JUND KLF3 SPIB STAT2
E
N1 N2 N3 N4 C1 C2 C3 C4
PML STAT2 STAT1 FOXK1 NFKB2 CDX2 HSF1 YAP1 XRN2 SUMO2 DDX5 OGT YY1
2 1 0 -1 -2
F
N1 N2 N3 N4 C1 C2 C3 C4
CREB1 S142
SMARCA4 T1423
YAP1 S109
PRKDC S893
CDK12 T1244
FOXK1 S101
XRN2 S448
MYH11 S638
ARRB1 S412
CBX3 S176
ARID1A S1755
LMNB1 S23
HCFC1 S1507
RING1 S38
2 1 0 -1 -2
G
The ratio of all the up-regulated NCMGs
NFKB2 YAP1 YY1 STAT1 OGT DDX5 SUMO2 FOXK1 STAT2 PML HSF1 CDX2 XRN2
H
The ratio of all the diff-exp NCMGs
CREB1 ARID1A CDK12 LMNB1 MYH11 YAP1 HCFC1 FOXK1 SMARCA4 CBX3 RING1 XRN2 PRKDC ARRB1
I
12 1 11
STAT2
J
10 3 11
YAP1
XRN2
FOXK1

Figure 3. Multiplatform analyses disclosing key transcriptional factors that potentially regulate NCMGs in human CRC. Transcriptional factors of NCMGs reflected by binding motifs in (A) normal and (B) CRC tissues, and the proportion of potentially targeted differentially expressed NCMGs of all the (C) down-regulated or (D) up-regulated NCMGs. Potential transcriptional factors of NCMGs were altered on (E) the protein level and (F) phosphorylation level, and the proportion of potentially targeted differentially expressed NCMGs of all the (G) up-regulated or (H) all altered NCMGs. (I) Venn analyses of the transcriptional factors listed in (A, B and E). (J) Venn analyses of transcriptional factors listed in (E and F).

function, including GLISI, JUN, NFKR2, CREB1, YAP1, STAT2, XRN2, and FOXK1.

Phosphoproteomic investigations uncovered potential key roles of p38 in mitochondrial activities in CRC and revealed networks among key kinases and transcriptional factors

To explore posttranslational modifications of mitochondrial proteins with potential impacts on protein activities, we examined eight CRC samples via phosphoproteomics analysis. The results showed that phosphorylation of 164 proteins was up-regulated and of 284 proteins was down-regulated, while 188 phosphorylation sites were up-regulated and 399 were down-regulated (**Figure 4A**). Through KEGG enrichment analysis of up-regulated proteins, pathways associated with bacteria were enriched and found to be altered to the greatest degree (**Figure 4B**), suggesting that bacterial inflammation was associated with CRC in this study, as previously reported for CRC patients [17, 18]. Notably, subcellular enrichment analysis revealed that nuclear proteins exhibited the greatest changes in the CRC group (**Figure 4C**) and accounted for 53% of all differentially phosphorylated proteins, thus suggesting that nuclear proteins changed dramatically during carcinogenesis. Meanwhile, we observed that 18 mitochondrial proteins were distinctively phosphorylated in CRC samples (**Figure 4D**), as depicted within a network of mitochondrial and other proteins undergoing phospho-modification (**Figure 4E**). Importantly, MCODE calculations revealed the closely-tied module in the above network, in which mitochondrial protein ARCN1 was found (**Figure 4F**).

Due to the fact that kinases are relevant to the phosphorylation of proteins, we screened 23 kinases that were differentially phosphorylated and found that 16 kinases were associated with mitochondrial regulation (Table S1). After scoring these kinases using the Cytoscape plug-in cytoHubba to assess their importance, we identified the top ten central kinases as *MAPK14*, *EGFR*, *PTK2*, *PTK2B*, *PAK1*, *RIPK1*, *MAP2K3*, *PRKCD*, *PRKDC*, and *GSK3B* (**Figure 5A-C**).

Notably, all of these kinases exhibited down-regulated phosphorylation. Additionally, phosphorylation of p38 (*MAPK14*) and its specific upstream kinase MKK3 (*MAP2K3*) were both down-regulated [19], suggesting that this pathway was inhibited in CRC. Due to the fact that we had observed a dramatic alteration of nucleoproteins in CRC (Figures S3, **4C**) and a high association between chromatin accessibility and patient survival (**Figure 2I**, **2L**), we speculated that upstream genes regulating mitochondrial functions were at least partially regulated through chromatin modification. Therefore, we searched for genes involved in modification of both mitochondria and chromatin (DNA replication, transcription, epigenetic modification, and chromatin remodeling) among all phosphorylation-altered CRC genes. Subsequently, differential phosphorylation of 15 genes was discovered (**Figure 5D**), with *MAPK14* and *GSK3B* found in this group (**Figure 5D**). Because p38 was singled out in two phosphorylation analyses while having the highest score, down-regulation of phosphorylation of p38 at Y182 might be an important factor underlying decreased mitochondrial activities observed in patients with bacteria-associated CRC (**Figure 5E**, **5F**). Next, we mapped proteins linked to p38 from the total pool of all identified differentially-phosphorylated genes (**Figure 5G**), and conducted the network of kinases and transcriptional factors shown in **Figure 5H**.

Notably, phosphorylation of RPTOR, an indispensable component of the mTORC1 complex, was significantly reduced at Ser863 (**Figure 5D**). This site had been previously reported to be involved in kinase activity and influence mTORC1 complex activity [20]. Meanwhile, several other reports have shown that RPTOR deficiency leads to decreased mitochondrial activity in T cells [21], suggesting that RPTOR plays an essential role in mitochondrial regulation. Intriguingly, RPTOR deficiency triggers tumor initiation in mice with colitis, implying that

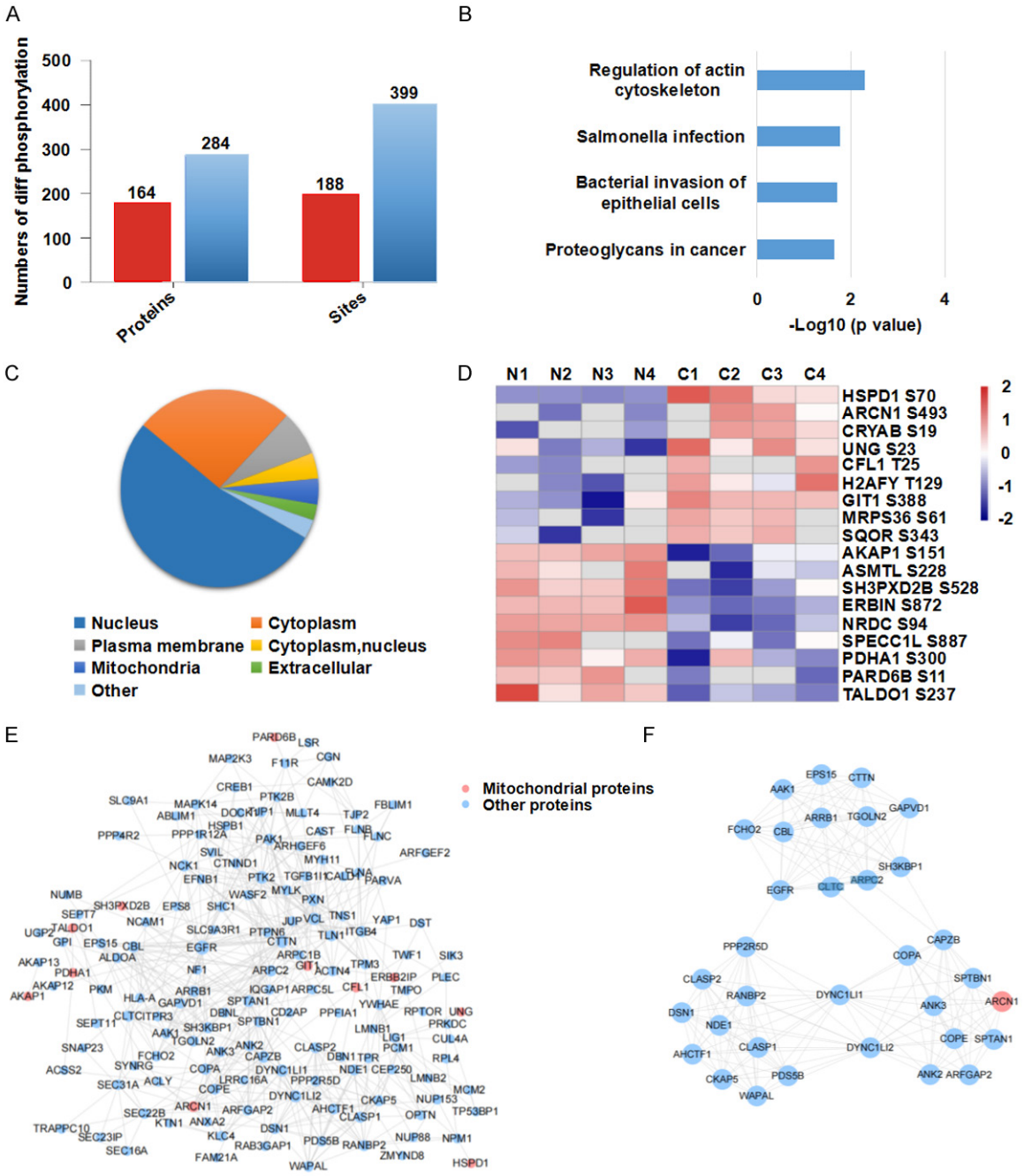

Figure 4. Phosphoproteomic investigations revealing distinctive phosphorylation modifications of mitochondrial proteins and interconnectivity among them. (A) Distinct phosphorylation modifications in CRC mitochondria detected via the phosphoproteomic analyses. (B) KEGG and (C) subcellular enrichment analyses of differentially expressed genes. (D) Unique phosphorylation of NCMGs in CRC patients. Genes with a fold change > 1.5 were regarded the differentially expressed genes. Networks of (E) phosphorylation-modified mitochondrial proteins with other proteins, and (F) the most closely-related group.

RPTOR or the mTORC1 complex act as suppressors during early-stage CRC [22]. Therefore, we further analyzed RPTOR phosphorylation at Ser863 during different CRC stages and found significantly reduced phosphorylation of RPTOR Ser863 during CRC initiation, with phosphoryla-

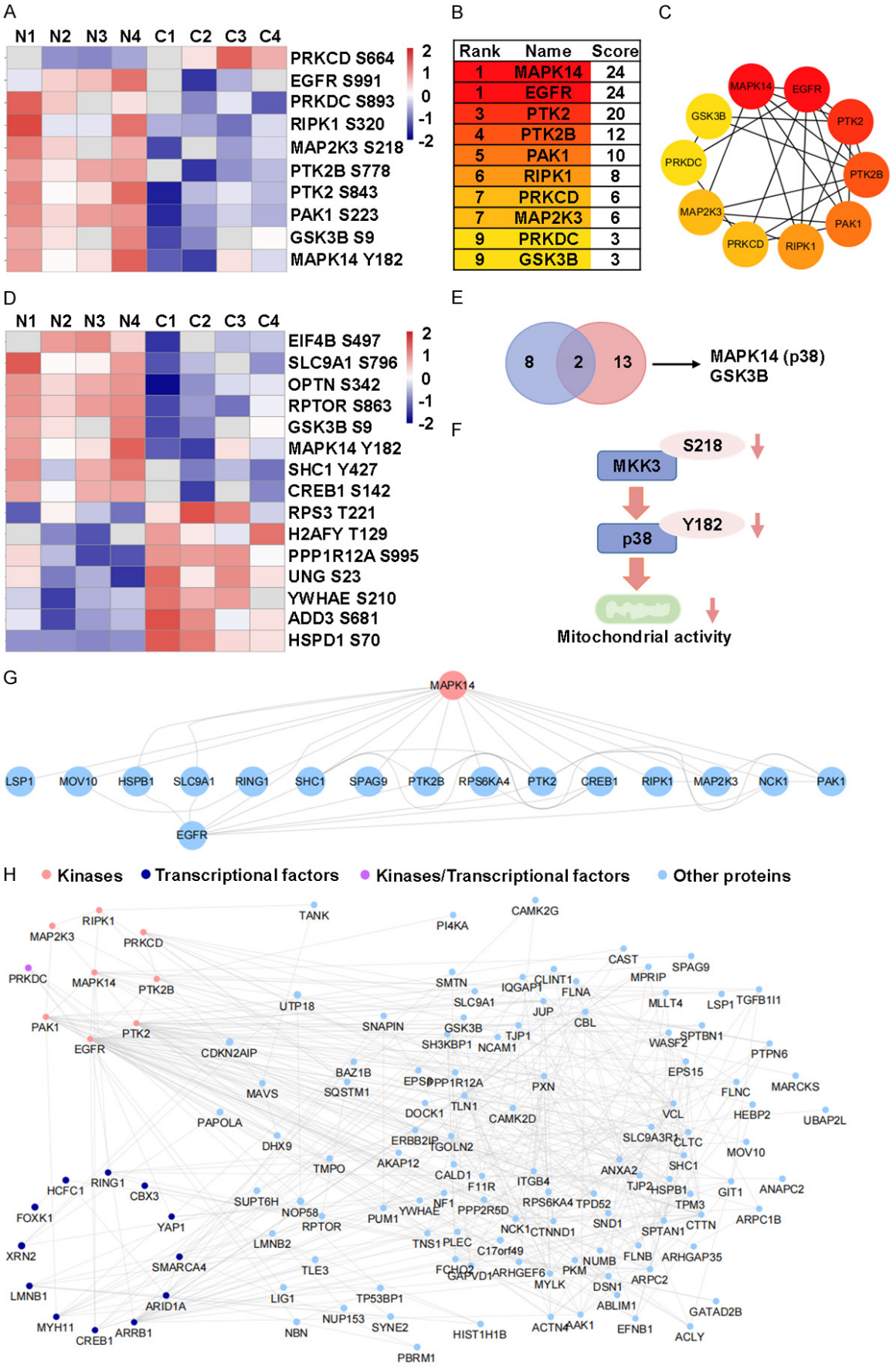
A
N1 N2 N3 N4 C1 C2 C3 C4
PRKCD S664
EGFR S991
PRKDC S893
RIPK1 S320
MAP2K3 S218
PTK2B S778
PTK2 S843
PAK1 S223
GSK3B S9
MAPK14 Y182
2
1
0
-1
-2
B
Rank Name Score
1 MAPK14 24
1 EGFR 24
3 PTK2 20
4 PTK2B 12
5 PAK1 10
6 RIPK1 8
7 PRKCD 6
7 MAP2K3 6
9 PRKDC 3
9 GSK3B 3
C
MAPK14
EGFR
GSK3B
PTK2
PRKDC
PTK2B
MAP2K3
PAK1
PRKCD
RIPK1
D
N1 N2 N3 N4 C1 C2 C3 C4
EIF4B S497
SLC9A1 S796
OPTN S342
RPTOR S863
GSK3B S9
MAPK14 Y182
SHC1 Y427
CREB1 S142
RPS3 T221
H2AFY T129
PPP1R12A S995
UNG S23
YWHAE S210
ADD3 S681
HSPD1 S70
2
1
0
-1
-2
E
8
2
13
MAPK14 (p38)
GSK3B
F
S218
MKK3
Y182
p38
Mitochondrial activity
G
MAPK14
LSP1
MOV10
HSPB1
SLC9A1
RING1
SHC1
SPAG9
PTK2B
RPS6KA4
PTK2
CREB1
RIPK1
MAP2K3
NCK1
PAK1
EGFR
H
Kinases
Transcriptional factors
Kinases/Transcriptional factors
Other proteins
TANK
CAMK2G
PI4KA
RIPK1
MAP2K3
PRKCD
PRKDC
MAPK14
PTK2B
UTP18
PAK1
PTK2
EGFR
CDKN2AIP
SNAPIN
SMTN
IQGAP1
CLINT1
FLNA
SLC9A1
JUP
CBL
GSK3B
TJP1
SH3KBP1
NCAM1
CAST
MPRIP
SPAG9
MLLT4
LSP1
TGFB1I1
WASF2
SPTBN1
PTPN6
EPS15
FLNC
MARCKS
HEBP2
UBAP2L
BAZ1B
EPS8
PPP1R12A
PXN
MAVS
SQSTM1
TLN1
DOCK1
CAMK2D
VCL
PAPOLA
DHX9
ERBB2IP
TGOLN2
SLC9A3R1
CLTC
MOV10
TMPO
AKAP12
CALD1
ANXA2
SHC1
HCFC1
RING1
CBX3
F11R
ITGB4
TJP2
HSPB1
GIT1
ANAPC2
SUPT6H
NOP58
YWHAE
NF1
PPP2R5D
RPS6KA4
TPD52
TPM3
FOXK1
YAP1
RPTOR
PUM1
NCK1
CTNND1
SND1
SPTAN1
CTTN
ARPC1B
XRN2
LMNB2
TNS1
PLEC
C17orf49
SMARCA4
TLE3
FCHO2
GAPVD1
ARHGEF6
MYLK
PKM
NUMB
FLNB
ARHGAP35
ARPC2
LMNB1
ARID1A
LIG1
TP53BP1
DSN1
ABLIM1
GATAD2B
MYH11
CREB1
ARRB1
NUP153
SYNE2
NBN
HIST1H1B
ACTN4
AAK1
EFNB1
ACLY
PBRM1

Figure 5. p38 as one of the central kinases potentially modulating mitochondrial activity in CRC patients. (A) Phosphorylation, (B) scores, and (C) networks of the differentially phosphorylated mitochondria-related kinases in CRC. (D) Phosphorylation of genes relevant to mitochondrial regulation and chromatin remodeling. (E) Venn analyses of genes listed in (A and D), with MAPK14 (p38) and GSK3B highlighted. (F) The pathway MKK3/p38 that regulates mitochondria in CRC. (G) Proteins directly linked to p38 and their network. (H) The network containing linkages among kinases, transcriptional factors, and differentially phosphorylated genes in CRC. "N" represents normal tissues and "C" represents cancer tissues. Genes with a fold change > 1.5 were regarded as differentially expressed genes.

tion gradually increasing during tumor development (Figure S4A). Thus, down-regulation of phosphorylation of RPTOR Ser863 might promote cellular transformation of CRC. Moreover, results we obtained from stage I-II CRC tumor sample phosphoproteome analysis revealed decreased phosphorylation of Ser1261 of mTOR, an upstream kinase that phosphorylated RPTOR Ser863 (Figure S4B) [23]. Meanwhile, phosphorylated mTOR Ser2448 was found to be completely absent in CRC (Figure S4C), a result that aligned with previous studies showing this residue to be relevant to RPTOR binding linked to malignancy [24, 25]. Furthermore, we investigated protein levels of RPTOR and MTOR using our own proteomic analyses and proteomic datasets representing 91 CRC patients that were obtained from the Tumor Characterization Program Proteogenomic Tumor Atlas of the Clinical Proteomic Tumor Analysis Consortium (CPTAC). Consequently, expression of RPTOR and MTOR were not significantly different between normal and CRC groups (Figure S5). We also obtained protein expression and phosphorylation results for proteins downstream of mTORC1, including 4E-BP1 and S6K. We found that 4E-BP1 was not expressed in normal and CRC tissues, while S6K was expressed at a slightly higher level in CRC but was not phosphorylated in CRC or normal groups. Therefore, these results indicate that inhibition of the mTORC1 pathway may occur in some patients and may have a role in promoting tumor initiation.

Discussion

In this study, proteomic analyses of eight human samples obtained from CRC tumors of patients at different CRC stages revealed that of all proteomes of organelles we studied, mitochondrial proteomes were altered most dramatically. Subsequent analysis of our original data combined with data of transcriptomic datasets obtained from the TCGA database led to identification of all mitochondria-associated IPFs with prognostic value for prediction of CRC patient outcomes. In addition, multiplatform analyses comparing mitochondrial alterations in CRC tissues versus healthy tissues included assessments of CRC-associated structural variants, DNA methylation changes, and chromatin accessibility differences, as well as results of proteomic and phosphoproteomic-based analyses (of mRNA, protein, phosphorylation and their interconnecting network) and alterations of vital transcriptional factors and kinases. Ultimately, the results demonstrated an association between mitochondrial dysregulation and CRC (**Figure 6**).

Currently over 50% of CRC patients are at risk of metastasis and recurrence, but no genetic prognostic biomarkers exist for use in identifying high-risk patients to guide development of appropriate treatment regimens [5]. Without treatment, the median survival time of CRC patients is only 5-10 months [5]. Reassuringly, multiplatform investigations combined with bioinformatics analyses may facilitate screening of potential prognostic genes to reveal factors with clinical value [10-12]. In our study, five potentially useful prognostic mitochondrial genes were discovered: *HIGD1A*, *CHDH*, *SLC25A24*, *SUCLG2*, and *TIMP1*. Notably, we found that expression levels of *HIGD1A*, *SLC25A24*, and *SUCLG2* decreased from colitis stage and continuously decreased with progression of disease from early to middle to late stages of CRC. Thus, these three genes might serve as CRC prognostic markers for use during all disease stages.

Due to mitochondrial roles that drive tumorigenesis, drugs targeting mitochondrial functions have attracted the attention of many researchers [26, 27]. The mitochondria-targeting drug ABT-199 (a BCL2-specific agent) has received Food and Drug Administration (FDA) approval for use in treatment of chronic/small lymphoblastic leukemia. However, ABT-737 (a BCL2/Bcl-XL dual inhibitor) as a CRC treatment has been tested in preclinical trials, with no FDA-approved drug yet in clinical use [26, 27].

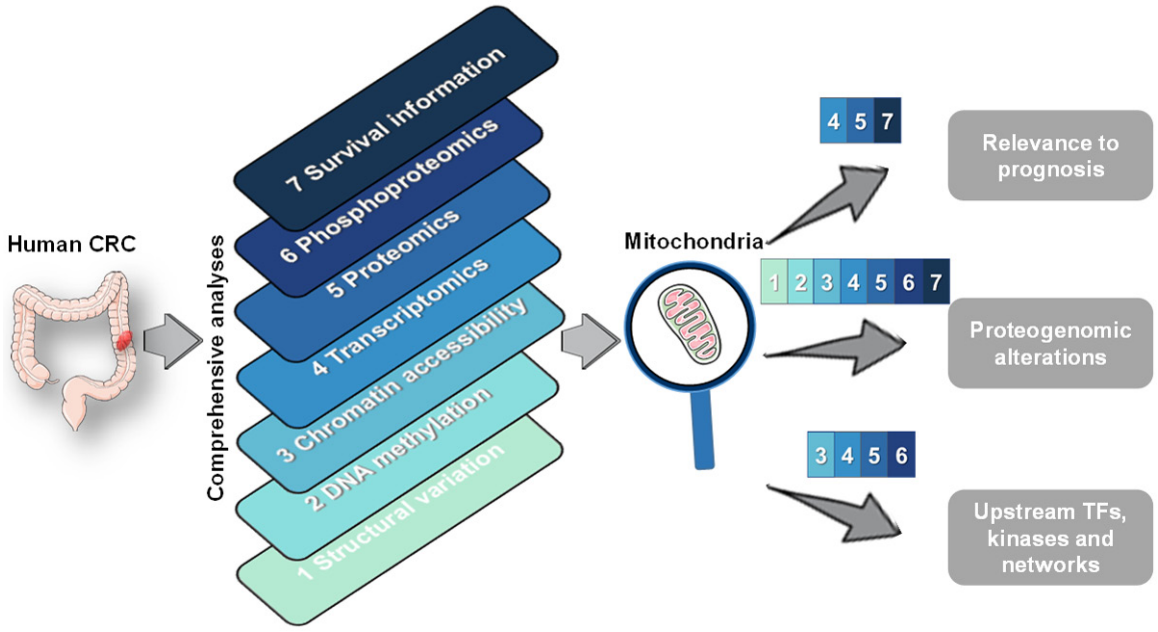

Figure 6. Graphical abstract of this research. Through a multi-omics study of human CRC tissues, we depicted mitochondrial alterations on distinct molecular levels and identified the information stream from DNA to RNA to protein to patient prognosis while also revealing potentially crucial regulatory transcriptional factors, kinases, and connective networks among them.

Therefore, screening to detect CRC-related mitochondrial genes, exploration of mechanisms whereby they induce CRC disease pathogenesis, and development of drugs targeting these mitochondrial genes are needed. In this project, we researched mitochondria-associated genes using a multiplatform analysis approach that included assessments of DNA, mRNA, and protein, as well as of epigenetic modifications and of potentially pathogenic mitochondrial genes, including *HIGD1A*, *SLC25A24*, *SUCLG2*, *CHDH*, *TFB1M*, *CHDH, MIPEP*, *PYCR2*, *LARS2*, and *PAICS*. Possible mechanisms underlying abnormal mitochondrial gene expression or associated modifications were also explored. The results we obtained provide insights into mechanisms underlying CRC disease and provide a theoretical basis to guide the development of gene therapy and treatment drugs.

As key organelles in eukaryotic cells, mitochondria are exclusively important for energy generation, metabolism, cell cycle processes, apoptosis, and microenvironmental adaptation. Our knowledge of mitochondrial links to cancer dates back to the 1850s, when the "Warburg hypothesis" declared tumor cells as possible results of aerobic glycolysis [6, 7]. To date, mitochondria have been recognized as both activators and inhibitors of carcinogenesis, depending on cancer stage and disease context [28-30]. In some tumors, numbers of mitochondria are elevated, such as in breast and thyroid cancers; however, in other tumors reduced numbers of mitochondria are observed, such as in colon, liver and lung cancers [6, 7, 30-32]. Notably, carcinogenic and cancer-suppressive pathways have both been found upstream of mitochondrial pathways, including those involving the mTOR oncogenic complex and suppressor p53, respectively [31]. In CRC pathogenesis, mitochondrial activities are impaired at early tumor initiation [6, 9], with subsequent changes in the metabolic microenvironment promoting cellular transformation and tumor development. By contrast, late-phase CRC cells require functioning mitochondria for survival, due to their requirements for energy to power cell proliferation. From our proteomic and phosphoproteomic results, we observed that 85.4% of differentially expressed NCMGs were down-regulated, and lower levels of phosphorylation of the top ten mitochondria-regulated kinases that possibly led to repression of these pathways. Taken together, these

results demonstrate that a dramatic loss of mitochondrial functions during CRC.

In addition, we found that human cells regulate transcription at various levels, including via opening or closing binding motifs on DNA, and modulating protein synthesis and phosphorylation levels of transcriptional factors. Indeed, we speculate that genes that are modulated via multiple levels of regulation are likely to play important roles in disease development. Based on this speculation, we uncovered potentially crucial transcription factors that participate in mitochondrial activities, such as YAP1, STAT2, XRN2, and FOXK1. Among them, YAP1 is well-known for its effects on metabolism and mitochondrial biogenesis [33, 34], but the roles of STAT2, XRN2, and FOXK1 in mitochondrial functions have not been fully studied. Previous reports have indicated that mutated STAT2 caused mitochondrial elongation observed in CRC tumor cells [35]. Notably, our research demonstrated higher STAT2 expression levels and greater numbers of its DNA binding motifs in CRC cells than in healthy cells, which implied that more STAT2 might be needed by CRC cells as compared to healthy cells.

In this study, we observed decreased phosphorylation of p38 at Thy 182 in CRC patient cells; this result is notable, since proteomic analyses have pinpointed p38 as the key kinase involved in mitochondrial regulation. As a serine/threonine kinase, p38 plays an important central role in regulating the cascade of cellular responses triggered by extracellular stimuli, such as pro-inflammatory cytokines or physical stress, thereby directly activating downstream transcriptional factors. In fact, p38 substrates include a wide range of proteins that include approximately 200 to 300 proteins [36]. With regard to CRC, it has been found that the p38 pathway plays dual roles in tumorigenesis, acting as a suppressor of cell proliferation, while activating metabolism, invasion, and angiogenesis [36]. Previous studies have shown that activation of p38 is positively involved in mitochondrial biogenesis and mitochondria-dependent apoptosis [37-40]. In normal tissues p38 promotes mitochondrial biogenesis that depends on cGMP-dependent induction [37], while in cancers, p38 initiates mitochondria-related transcription through partial phosphorylation of PGC-1α [38]. Meanwhile, MKK3 acts as a specific upstream kinase of p38 and has been reported to participate in mitochondrial modulation, as evidenced by the fact that MKK3-deficient mice exhibit mitochondrial dysfunction [41]. Consistent with these findings, our investigations here demonstrated that p38 inactivation was potentially associated with mitochondrial loss in CRC.

Interestingly, we found lower levels of phosphorylation of RPTOR at Ser863 and mTOR at Ser1261 and Ser2448, as had been reported previously in a large study of CRC samples with microsatellite instability (MSI) [12]. More specifically, the activity of mTORC1 appeared to be down-regulated in our CRC patient samples, in spite of the fact that about 50% of cancer patients have been shown to exhibit activated mTORC1 [42-44]. For a long time, RPTOR and mTORC1 were widely considered to be tumor promoters [45-47], prompting studies exploring the potential efficacy of mTORC1 inhibitors for use in tumor therapy. However, limited efficacy has been found for any single agent [48-50]. For example, in a rapalog evaluation study, only 1 of 28 patients experienced a positive response to treatment [50, 51]. As revealed by our experiments, natural inhibition of mTORC1 activity observed in some CRC patients may align with results showing moderate efficacy of mTORC1 antagonists as observed in clinical trials. Notably, several recent studies have revealed a tumor-suppressive role for mTORC1 during the initial stage of cancer in that inactivation of mTORC1 led to cellular transformation in mice with colitis [22, 52], while a RPTOR deficiency induced hepatocarcinogenesis in mice [51]. Therefore, suppression of mTORC1 activity via treatment of CRC patients with inhibitors may not impair tumors and may even accelerate carcinogenesis in some cases. Clinically, antagonists of mTORC1, such as rapamycin, have been widely used to achieve immunosuppression after organ transplantation [53, 54]; however, our research suggests that use of mTORC1 inhibitors for immunosuppression or cancer treatment should be customized to each patient, and it may not be applicable to patients with enteritis and hepatitis.

In summary, we discovered that mitochondria function as vital organelles during tumorigenesis and are strongly tied to CRC patient prognosis. Moreover, we provided the first survival-related proteogenomic depiction of mitochondria in human CRC, with roles of regulatory

genes in mitochondrial activity and connectivity among them also described. These findings would enhance our knowledge of mitochondrial roles in CRC pathogenesis and progression and would facilitate discovery of new biomarkers and target genes with clinical value.

Acknowledgements

This work was supported by the Science and Technology Planning Project of Guangdong Province, China (No. 2017B020209001), the Key Research and Development Program of Guangdong Province (No. 2019B020229001), the National Natural Science Foundation of China (No. 81671596, No. 82003172), the Guangdong Basic and Applied Basic Research Foundation (No. 2019A1515111138) and China Postdoctoral Science Foundation (2020-M673065).

Disclosure of conflict of interest

None.

Address correspondence to: Lianghong Yin, Department of Nephrology, Institute of Nephrology and Blood Purification, The First Affiliated Hospital of Jinan University, Jinan University, Guangzhou 510-632, China. E-mail: yin-yun@126.com; Yong Xu, The First Affiliated Hospital of Shenzhen University, Shenzhen Second People's Hospital, Shenzhen 518028, China. E-mail: xuyong_2000@tom.com; Yong Dai, Department of Clinical Medical Research Center, The Second Clinical Medical College of Jinan University, The First Affiliated Hospital Southern University of Science and Technology, Shenzhen People's Hospital, Shenzhen 518020, China. Tel: +86-0755-22942780; Fax: +86-0755-22942780; E-mail: daiyong22@aliyun.com

References

[1] Dekker E, Tanis PJ, Vleugels JLA, Kasi PM and Wallace MB. Colorectal cancer. Lancet 2019; 394: 1467-1480.

[2] Rawla P, Barsouk A, Hadjinicolaou AV and Barsouk A. Immunotherapies and targeted therapies in the treatment of metastatic colorectal cancer. Med Sci (Basel) 2019; 7: 83.

[3] Ganesh K, Stadler ZK, Cercek A, Mendelsohn RB, Shia J, Segal NH and Diaz LA Jr. Immunotherapy in colorectal cancer: rationale, challenges and potential. Nat Rev Gastroenterol Hepatol 2019; 16: 361-375.

[4] Siegel RL, Miller KD, Goding Sauer A, Fedewa SA, Butterly LF, Anderson JC, Cercek A, Smith RA and Jemal A. Colorectal cancer statistics, 2020. CA Cancer J Clin 2020; 70: 145-164.

[5] Lichtenstern CR, Ngu RK, Shalapour S and Karin M. Immunotherapy, inflammation and colorectal cancer. Cells 2020; 9: 618.

[6] Jackson DN and Theiss AL. Gut bacteria signaling to mitochondria in intestinal inflammation and cancer. Gut Microbes 2020; 11: 285-304.

[7] Smolková K, Plecitá-Hlavatá L, Bellance N, Benard G, Rossignol R and Ježek P. Waves of gene regulation suppress and then restore oxidative phosphorylation in cancer cells. Int J Biochem Cell Biol 2011; 43: 950-968.

[8] Roth KG, Mambetsariev I, Kulkarni P and Salgia R. The mitochondrion as an emerging therapeutic target in cancer. Trends Mol Med 2020; 26: 119-134.

[9] Haberman Y, Karns R, Dexheimer PJ, Schirmer M, Somekh J, Jurickova I, Braun T, Novak E, Bauman L, Collins MH, Mo A, Rosen MJ, Bonkowski E, Gotman N, Marquis A, Nistel M, Rufo PA, Baker SS, Sauer CG, Markowitz J, Pfefferkorn MD, Rosh JR, Boyle BM, Mack DR, Baldassano RN, Shah S, Leleiko NS, Heyman MB, Griffiths AM, Patel AS, Noe JD, Aronow BJ, Kugathasan S, Walters TD, Gibson G, Thomas SD, Mollen K, Shen-Orr S, Huttenhower C, Xavier RJ, Hyams JS and Denson LA. Ulcerative colitis mucosal transcriptomes reveal mitochondriopathy and personalized mechanisms underlying disease severity and treatment response. Nat Commun 2019; 10: 38.

[10] Cancer Genome Atlas Network. Comprehensive molecular characterization of human colon and rectal cancer. Nature 2012; 487: 330-337.

[11] Zhang B, Wang J, Wang X, Zhu J, Liu Q, Shi Z, Chambers MC, Zimmerman LJ, Shaddox KF, Kim S, Davies SR, Wang S, Wang P, Kinsinger CR, Rivers RC, Rodriguez H, Townsend RR, Ellis MJ, Carr SA, Tabb DL, Coffey RJ, Slebos RJ and Liebler DC. Proteogenomic characterization of human colon and rectal cancer. Nature 2014; 513: 382-387.

[12] Vasaikar S, Huang C, Wang X, Petyuk VA, Savage SR, Wen B, Dou Y, Zhang Y, Shi Z, Arshad OA, Gritsenko MA, Zimmerman LJ, McDermott JE, Clauss TR, Moore RJ, Zhao R, Monroe ME, Wang YT, Chambers MC, Slebos RJC, Lau KS, Mo Q, Ding L, Ellis M, Thiagarajan M, Kinsinger CR, Rodriguez H, Smith RD, Rodland KD, Liebler DC, Liu T and Zhang B. Proteogenomic analysis of human colon cancer reveals new therapeutic opportunities. Cell 2019; 177: 1035-1049, e1019.

[13] van de Wetering M, Francies HE, Francis JM, Bounova G, Iorio F, Pronk A, van Houdt W, van Gorp J, Taylor-Weiner A, Kester L, McLaren-Douglas A, Blokker J, Jaksani S, Bartfeld S, Vol-

ckman R, van Sluis P, Li VS, Seepo S, Sekhar Pedamallu C, Cibulskis K, Carter SL, McKenna A, Lawrence MS, Lichtenstein L, Stewart C, Koster J, Versteeg R, van Oudenaarden A, Saez-Rodriguez J, Vries RG, Getz G, Wessels L, Stratton MR, McDermott U, Meyerson M, Garnett MJ and Clevers H. Prospective derivation of a living organoid biobank of colorectal cancer patients. Cell 2015; 161: 933-945.

[14] Meier F, Brunner AD, Koch S, Koch H, Lubeck M, Krause M, Goedecke N, Decker J, Kosinski T, Park MA, Bache N, Hoerning O, Cox J, Räther O and Mann M. Online Parallel Accumulation-Serial Fragmentation (PASEF) with a novel trapped ion mobility mass spectrometer. Mol Cell Proteomics 2018; 17: 2534-2545.

[15] Buenrostro JD, Wu B, Chang HY and Greenleaf WJ. ATAC-seq: a method for assaying chromatin accessibility genome-wide. Curr Protoc Mol Biol 2015; 109: 21.29.21-21.29.29.

[16] Theocharopoulou G. The ubiquitous role of mitochondria in Parkinson and other neurodegenerative diseases. AIMS Neurosci 2020; 7: 43-65.

[17] Wang L, Tang L, Feng Y, Zhao S, Han M, Zhang C, Yuan G, Zhu J, Cao S, Wu Q, Li L and Zhang Z. A purified membrane protein from Akkermansia muciniphila or the pasteurised bacterium blunts colitis associated tumourigenesis by modulation of CD8(+) T cells in mice. Gut 2020; 69: 1988-1997.

[18] Baker AM, Cross W, Curtius K, Al Bakir I, Choi CR, Davis HL, Temko D, Biswas S, Martinez P, Williams MJ, Lindsay JO, Feakins R, Vega R, Hayes SJ, Tomlinson IPM, McDonald SAC, Moorghen M, Silver A, East JE, Wright NA, Wang LM, Rodriguez-Justo M, Jansen M, Hart AL, Leedham SJ and Graham TA. Evolutionary history of human colitis-associated colorectal cancer. Gut 2019; 68: 985-995.

[19] Stramucci L, Pranteda A and Bossi G. Insights of crosstalk between p53 protein and the MKK3/MKK6/p38 MAPK signaling pathway in cancer. Cancers (Basel) 2018; 10: 131.

[20] Foster KG, Acosta-Jaquez HA, Romeo Y, Ekim B, Soliman GA, Carriere A, Roux PP, Ballif BA and Fingar DC. Regulation of mTOR complex 1 (mTORC1) by raptor Ser863 and multisite phosphorylation. J Biol Chem 2010; 285: 80-94.

[21] Tan H, Yang K, Li Y, Shaw TI, Wang Y, Blanco DB, Wang X, Cho JH, Wang H, Rankin S, Guy C, Peng J and Chi H. Integrative proteomics and phosphoproteomics profiling reveals dynamic signaling networks and bioenergetics pathways underlying T cell activation. Immunity 2017; 46: 488-503.

[22] Brandt M, Grazioso TP, Fawal MA, Tummala KS, Torres-Ruiz R, Rodriguez-Perales S, Perna C and Djouder N. mTORC1 inactivation promotes colitis-induced colorectal cancer but protects from APC loss-dependent tumorigenesis. Cell Metab 2018; 27: 118-135, e118.

[23] Wang L, Lawrence JC Jr, Sturgill TW and Harris TE. Mammalian target of rapamycin complex 1 (mTORC1) activity is associated with phosphorylation of raptor by mTOR. J Biol Chem 2009; 284: 14693-14697.

[24] Rosner M, Siegel N, Valli A, Fuchs C and Hengstschläger M. mTOR phosphorylated at S2448 binds to raptor and rictor. Amino Acids 2010; 38: 223-228.

[25] Lisi L, Ciotti GMP, Chiavari M, Pizzoferrato M, Mangiola A, Kalinin S, Feinstein DL and Navarra P. Phospho-mTOR expression in human glioblastoma microglia-macrophage cells. Neurochem Int 2019; 129: 104485.

[26] Chiu HY, Tay EXY, Ong DST and Taneja R. Mitochondrial dysfunction at the center of cancer therapy. Antioxid Redox Signal 2020; 32: 309-330.

[27] Russell OM, Gorman GS, Lightowlers RN and Turnbull DM. Mitochondrial diseases: hope for the future. Cell 2020; 181: 168-188.

[28] Sepulveda-Villegas M, Rojo R, Garza-Hernandez D, de la Rosa-Garza M and Treviño V. A systematic review of genes affecting mitochondrial processes in cancer. Biochim Biophys Acta Mol Basis Dis 2020; 1866: 165846.

[29] Vyas S, Zaganjor E and Haigis MC. Mitochondria and cancer. Cell 2016; 166: 555-566.

[30] Zong WX, Rabinowitz JD and White E. Mitochondria and cancer. Mol Cell 2016; 61: 667-676.

[31] Moreno-Sánchez R, Rodríguez-Enríquez S, Marín-Hernández A and Saavedra E. Energy metabolism in tumor cells. FEBS J 2007; 274: 1393-1418.

[32] Chatterjee A, Mambo E and Sidransky D. Mitochondrial DNA mutations in human cancer. Oncogene 2006; 25: 4663-4674.

[33] Koo JH and Guan KL. Interplay between YAP/TAZ and metabolism. Cell Metab 2018; 28: 196-206.

[34] Mammoto A, Muyleart M, Kadlec A, Gutterman D and Mammoto T. YAP1-TEAD1 signaling controls angiogenesis and mitochondrial biogenesis through PGC1α. Microvasc Res 2018; 119: 73-83.

[35] Shahni R, Cale CM, Anderson G, Osellame LD, Hambleton S, Jacques TS, Wedatilake Y, Taanman JW, Chan E, Qasim W, Plagnol V, Chalasani A, Duchen MR, Gilmour KC and Rahman S. Signal transducer and activator of transcrip-

tion 2 deficiency is a novel disorder of mitochondrial fission. Brain 2015; 138: 2834-2846.
[36] Grossi V, Peserico A, Tezil T and Simone C. p38α MAPK pathway: a key factor in colorectal cancer therapy and chemoresistance. World J Gastroenterol 2014; 20: 9744-9758.
[37] Bhargava P, Janda J and Schnellmann RG. Elucidation of cGMP-dependent induction of mitochondrial biogenesis through PKG and p38 MAPK in the kidney. Am J Physiol Renal Physiol 2020; 318: F322-F328.
[38] Chaube B, Malvi P, Singh SV, Mohammad N, Viollet B and Bhat MK. AMPK maintains energy homeostasis and survival in cancer cells via regulating p38/PGC-1α-mediated mitochondrial biogenesis. Cell Death Discov 2015; 1: 15063.
[39] Huang CH, Lee YC, Chiou JT, Shi YJ, Wang LJ and Chang LS. Arsenic trioxide-induced p38 MAPK and Akt mediated MCL1 downregulation causes apoptosis of BCR-ABL1-positive leukemia cells. Toxicol Appl Pharmacol 2020; 397: 115013.
[40] He W, Li Y, Tian J, Jiang N, Du B and Peng Y. Optimized mixture of As, Cd and Pb induce mitochondria-mediated apoptosis in C6-glioma via astroglial activation, inflammation and P38-MAPK. Am J Cancer Res 2015; 5: 2396-2408.
[41] Srivastava A, Shinn AS, Lee PJ and Mannam P. MKK3 mediates inflammatory response through modulation of mitochondrial function. Free Radic Biol Med 2015; 83: 139-148.
[42] Sobočan M, Bračič S, Knez J, Takač I and Haybaeck J. The communication between the PI3K/AKT/mTOR pathway and Y-box binding protein-1 in gynecological cancer. Cancers (Basel) 2020; 12: 205.
[43] Bhat M, Sonenberg N and Gores GJ. The mTOR pathway in hepatic malignancies. Hepatology 2013; 58: 810-818.
[44] Khan MA, Jain VK, Rizwanullah M, Ahmad J and Jain K. PI3K/AKT/mTOR pathway inhibitors in triple-negative breast cancer: a review on drug discovery and future challenges. Drug Discov Today 2019; 24: 2181-2191.
[45] Murugan AK. mTOR: role in cancer, metastasis and drug resistance. Semin Cancer Biol 2019; 59: 92-111.
[46] Lu X, Paliogiannis P, Calvisi DF and Chen X. Role of the mammalian target of rapamycin pathway in liver cancer: from molecular genetics to targeted therapies. Hepatology 2021; 73 Suppl 1: 49-61.
[47] Foster KG and Fingar DC. Mammalian target of rapamycin (mTOR): conducting the cellular signaling symphony. J Biol Chem 2010; 285: 14071-14077.
[48] Kim DD and Eng C. The promise of mTOR inhibitors in the treatment of colorectal cancer. Expert Opin Investig Drugs 2012; 21: 1775-1788.
[49] Yang J, Nie J, Ma X, Wei Y, Peng Y and Wei X. Targeting PI3K in cancer: mechanisms and advances in clinical trials. Mol Cancer 2019; 18: 26.
[50] Zhu AX, Abrams TA, Miksad R, Blaszkowsky LS, Meyerhardt JA, Zheng H, Muzikansky A, Clark JW, Kwak EL, Schrag D, Jors KR, Fuchs CS, Iafrate AJ, Borger DR and Ryan DP. Phase 1/2 study of everolimus in advanced hepatocellular carcinoma. Cancer 2011; 117: 5094-5102.
[51] Umemura A, Park EJ, Taniguchi K, Lee JH, Shalapour S, Valasek MA, Aghajan M, Nakagawa H, Seki E, Hall MN and Karin M. Liver damage, inflammation, and enhanced tumorigenesis after persistent mTORC1 inhibition. Cell Metab 2014; 20: 133-144.
[52] Gutiérrez-Martínez IZ, Rubio JF, Piedra-Quintero ZL, Lopez-Mendez O, Serrano C, Reyes-Maldonado E, Salinas-Lara C, Betanzos A, Shibayama M, Silva-Olivares A, Candelario-Martinez A, Meraz-Ríos MA, Schnoor M, Villegas-Sepúlveda N and Nava P. mTORC1 prevents epithelial damage during inflammation and inhibits colitis-associated colorectal cancer development. Transl Oncol 2019; 12: 24-35.
[53] Nashan B. mTOR inhibition and clinical transplantation: liver. Transplantation 2018; 102: S19-S26.
[54] Nguyen LS, Vautier M, Allenbach Y, Zahr N, Benveniste O, Funck-Brentano C and Salem JE. Sirolimus and mTOR inhibitors: a review of side effects and specific management in solid organ transplantation. Drug Saf 2019; 42: 813-825.

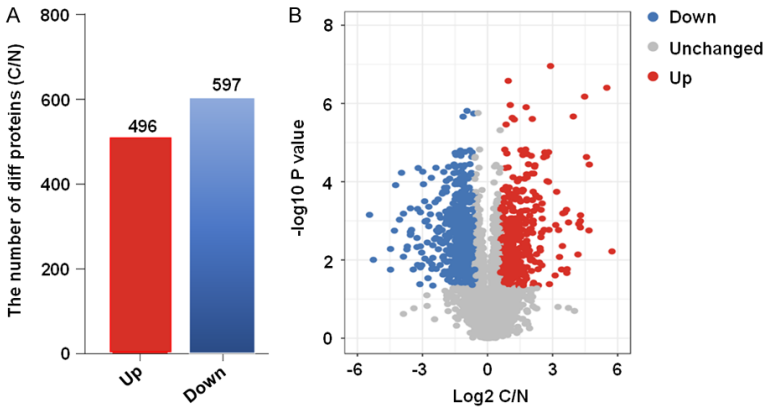

Figure S1. The differentially-expressed genes in CRC patients. (A) The histogram and (B) volcano plot showed 496 up-regulated and 597 down-regulated genes in CRC analyzed by proteomic investigations (Fold change > 1.5, P < 0.05). "C" indicated CRC tissues, and "N" indicated adjacent normal tissues. n = 8.

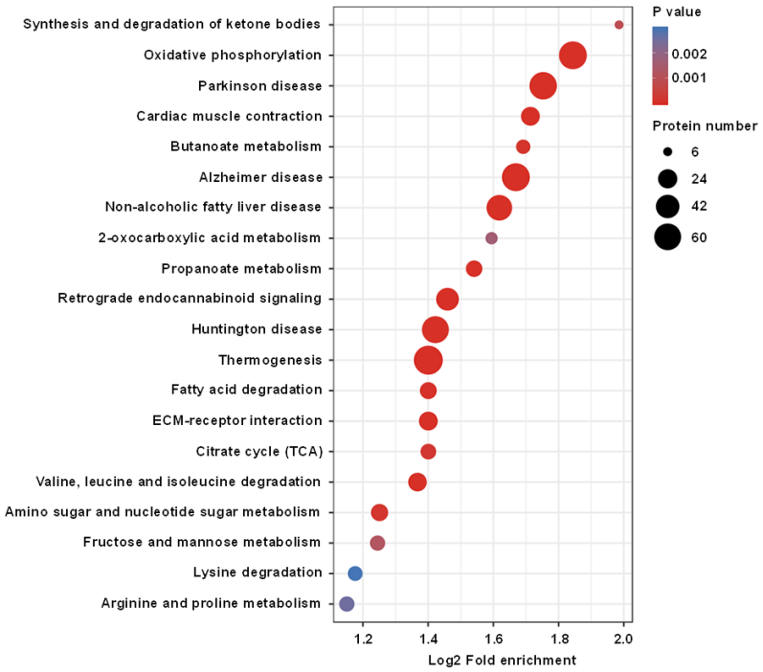

Figure S2. KEGG pathway enrichment proclaimed that mitochondria-relevant pathways were intensely related to the development of CRC.

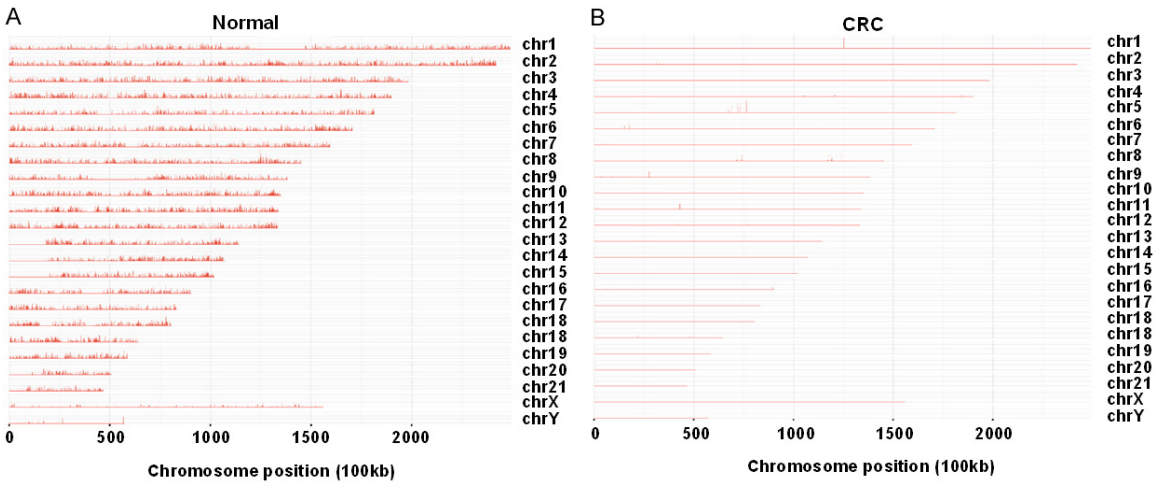

Figure S3. The accessible chromatin was massively decreased in CRC patients. The landscape of open chromatin of (A) adjacent normal and (B) CRC tissues. n = 6.

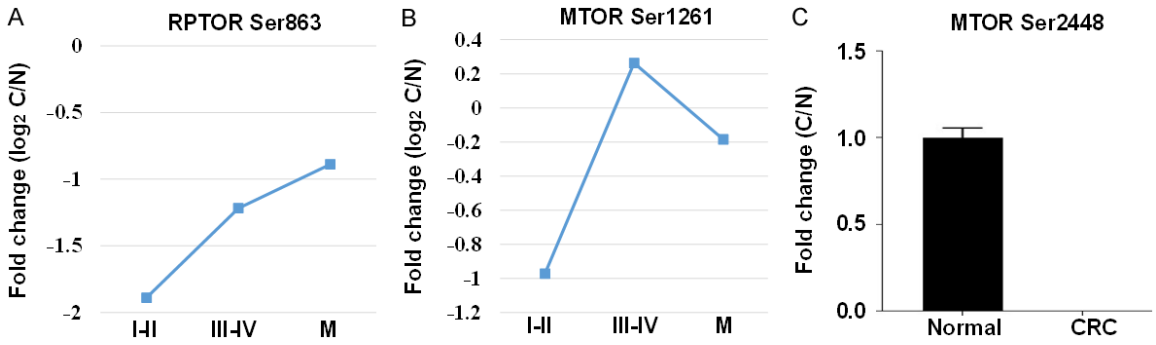

Figure S4. The phosphorylation of RPTOR and MTOR was down-regulated in early-phase CRC patients. (A) The phosphorylation of RPTOR at Ser863 and (B) MTOR at Ser1261 at different stages of CRC. "M" indicated III-IV patients with systemic metastases. $n_{I-II} = 4$; $n_{III-IV} = 2$; $n_{M} = 2$. (C) The phosphorylation of MTOR at Ser2448 in the normal and CRC tissues. n = 8.

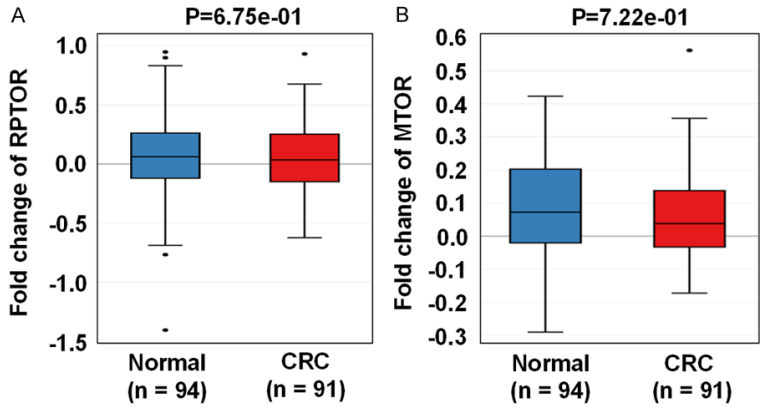

Figure S5. The protein levels of RPTOR and MTOR in CRC. The protein expression was analyzed through the datasets downloaded from the Tumor Characterization Program (Proteogenomic Tumor Atlas) database (CPTAC).